Reprinted from

Ninth International Symposium

Machine Processing of

Remotely Sensed Data

with special emphasis on

Natural Resources Evaluation

June 21-23, 1983

Proceedings

Purdue University
The Laboratory for Applications of Remote Sensing
West Lafayette, Indiana 47907 USA

A SUCCESSFUL APPROACH IN THREE-DIMENSIONAL PERCEPTION OF STEREO LANDSAT-MSS IMAGES OVER CORDILLERAN RELIEF

R. SIMARD, V.G. KRISHNA

Canada Centre for Remote Sensing
Ottawa, Canada

I ABSTRACT

Stereo images from LANDSAT MSS may be obtained on overlapping areas acquired from adjacent orbits. A methodology has been developed for extracting the parallax information from such images using a two stage image correlation technique to obtain digital elevation models. Algorithms and methodology used to model the terrain are described. The results, obtained using this technique for two test sites covering 3500 square kilometres, are presented.

II INTRODUCTION

LANDSAT-MSS data acquired from adjacent orbits generate steroscopic images with side-looking and near epipolar geometry. The small values of the slant angle (less than 5.8°) together with the relatively large pixel size of the MSS has considerably limited the use of such stereo pairs over Cordilleran type relief. However, previous works [1,2] have shown that parallax information exists in such images and can be measured, by using digital image processing techniques, to sub-pixel accurary.

A methodology has been developed to adapt a stereo correlation process to LANDSAT-MSS data and to generate digital elevation models (DEMs). These stereo correlation algorithms are able to measure very small amounts of parallax between stereo pairs (of the order of one fifth of a pixel) and this consequently provides a capability to determine relief with a resolution of a few hundred metres.

This technique has been developed after various tests have successfully measured the very small parallax between LANDSAT 2-MSS stereo images. The technique has been applied to a set of stereo images of moderate relief in British Columbia; the Kamloops test site (see Figures 1 and 2). These sub-scenes were obtained from overlapping images acquired within a 24 hour interval (frames corresponding to path-row 49-24 and 50-24) at latitude 55°N. They cover an area of 3500 square kilometres, with an altitude range of approximately 2000 metres. The headings of the two adjacent orbits are not parallel and thus call for a two-dimensional correlation scheme.

In order to simplify the stereo correlation algorithm to a quasi one dimensional process, these images have been rectified and resampled to 50 metre square pixels. These precision processed images are projected onto a Universal Transverse Mercator (UTM) grid by using ground control points extracted from 1:50 000 scale National Topographic System maps on the CCRS Digital Image Correction System (DICS) [3,4]. In these images, after alignment to the UTM grid, the parallax is predominant in the east-west direction (typically 98% for a heading of 192°), therefore the parallax estimation can be restricted to single dimension.

Figure 1 represents the MSS image (band 7) obtained from scene 50-24 while Figure 2 corresponds to scene 49-24. Three dimensional perception as seen under a stereoscope exhibits almost no relief. This is a consequence of the very small base to height ratio, of approximately 10% which generates parallax of only ±2 pixels over a mean altitude datum plane. This value corresponds to the parallax range input to the digital stereo correlation algorithm.

III DIGITAL ELEVATION MODELING

The elevation model is derived through three major steps (see Figure 3). The first is the evaluation of the parallax by means of digital correlation on the stereo pair. This measurement is restricted to one dimension (east-west) for simplicity and precision. This step is the most crucial one as small amounts of misregistration have to be measured accurately between small areas of different images.

The second step consists of deriving a geometric model to relate the east-west component of the parallax with elevation relative to an arbitrary datum plane. This is an analytical process, developed from known parameters such as the trace of the orbit, attitude, slant angle, earth curvature and tilt angle between orbits.

Finally the third step consists of absolute calibration of the elevation with actual altitude values extracted from topographic maps. These altimetric ground control points are used to model the effects of the low frequency variations in the relief, which could have been distorted by residual geometric errors at the pre-processing level.

A) STEREO CORRELATION ALGORITHM

The measurement of parallax from stereo images involves identifying, for each pixel in the first (reference) image, a corresponding pixel in the second image and measuring the difference in their coordinates. Various similarity measures can be used for identifying the corresponding pixels [5]. In this case statistical correlation coefficients are used to measure the similarity.

Figure 4 illustrates this process. I1 and I2 represent the two stereo images. For a pixel P in line L of I1, the location of the corresponding pixel P' in I2 is predicted from the parallax values of the pixel (P-1) in line L and pixel P in line (L-1). A source window W of J lines by K pixels is selected in the image I1 around pixel P. A search window S of size M lines by N pixels ($1 \leq J \leq M$, $1 \leq K \leq N$) is selected around P' in image I2. The correlation matrix R (M-J+1, N-K+1) is calculated by moving the source window W in the search window S. The windows are normalized to zero mean and the correlation coefficient is obtained using the formula:

$$R(p,q) = \frac{\sum_{j=1}^{J} \sum_{k=1}^{K} W(j,k)\, S(j+p,k+q)}{\left[\sum_{j=1}^{J} \sum_{k=1}^{K} W^2(j,k)\right]^{\frac{1}{2}} \left[\sum_{j=1}^{J} \sum_{k=1}^{K} S^2(j+p,k+q)\right]^{\frac{1}{2}}} \qquad (1)$$

The correlation matrix R is processed to find the local maximum, and the location of the point P in image I2 is determined to sub-pixel accuracy by interpolating the values around the correlation peak. The parallax is determined as the difference in coordinates of P in I1 and I2 and the parallax is translated to the corresponding elevation, overlaying the image I1, using a geometric model.

Some of the problems encountered during this process are:

(i) low variance among pixels in window W
(ii) weak local maximum in correlation matrix R
(iii) multiple local maxima in correlation matrix R
(iv) local maximum occurring at one of the edges in matrix R.

The first two problems can be attributed mainly to the uniformity in the image content in windows W and S and to the difference in the image content due to the multitemporal nature and different look angles for I1 and I2. The fourth problem occurs because of errors in the prediction of P' and can be overcome by repeating the procedure with P' at the new local maximum. The problem of multiple local maxima (also refered to as multiple peak problem) is quite crucial and could be due to image content and small source windows (small J and K). Increasing the size of the source window has a low pass filtering effect on the elevation component of the data and results in the loss of high frequency terrain information in the output. Also, it has been observed that the acceptance of the highest peak (in the case of multiple peaks) sometimes results in the selection of an incorrect point and the resulting parallax introduces errors in the output elevation contours. So in order to be confident of the parallax information, a two stage 'zoom-in' technique was adopted.

In the first stage, a larger source window (9x9 pixels) is selected and the pixel P is located in the image I2. In the second stage correlation is done on horizontal gradients by choosing smaller source (5x5 pixels) and search windows, around the point identified in the first stage. The exact location of P is determined by interpolating the correlation coefficient around the local maximum. The first stage provides an approximate location of pixel P reliably and the smaller window size in the second stage facilitates the calculation of the parallax to subpixel accuracy without filtering out high frequency. Also, the points, at which low variance, low peak and multiple peak problems are detected, are ignored. The elevations at these points are interpolated in the output from neighbouring good points. Figure 5 describes the various steps involved in the overall process.

The image correlation process discussed here differs from the other algorithms as discussed by Barnea and Silverman [5], as it employs a two stage process. The two stage process is necessitated by the restriction on the large window sizes which would destroy the high frequency elevation information. Also, elimination of errors due to misregistration is crucial as this would introduce errors in the output elevation contours. So each point whose correlation matrix contains low peak or multiple peaks, is ignored in the parallax measurement process. The two stage zoom-in technique provides reliability and accuracy to the parallax measurement [6].

As discussed previously parallax in these stereo pairs, being predominant in the east-west direction, is measured in that direction only. However, a two dimensional correlation is done first to determine the exact line on which the source window registers with the search window. As the DICS product is resampled to 50 metres in the line direction from an original 79 metre pixel, alternate lines are used while selecting source and search windows. This undersampling ensures effective line registration without using large window sizes in the line direction. It has been observed that without this line skip process, the peaks in the line direction are not sharp and thus introduce a certain amount of uncertainty in the line registration.

B) GEOMETRIC MODELING

A geometric model has been constructed relating the parallax of a given point in the east-west direction (Px) to the elevation h at this point. The relationship is basically linear in a simple model which includes only the base to satellite height ratio and the orientation of the mean heading of the two orbits.

The relationship becomes slightly modified when the effects of the non-parallel headings of the adjacent orbits and earth curvature are considered. Figure 6 shows the variation of Px as a percentage of elevation when the effects of non-parallel headings and earth curvature are taken into account. The variation is about 0.25% and is contributed mainly by the difference in heading of the adjacent orbits (going south-west, the base between traces of orbits is increasing).

IV RESULTS

The Figure 7 represents the map of the elevation extracted from LANDSAT and defined relative to an arbitrary datum plane. The increment between contours is 250 metres. This map is registered with the image acquired from frame 50-24 (see Figure 1) which has been taken as a planimetric reference for the parallax and corresponding height location. The digital elevation model is extracted over a grid of 200 metres and resampled to 50 metres to overlay the corresponding LANDSAT image. As no values are extracted on lakes and rivers, no contours define the shore lines. The large dimensions of the correlator window (500 m x 250 m) act as a low pass filter on the elevation and introduce artifacts on lake and river shore lines.

The correlation results for the test site are presented in Table 1. The first row gives the correlation results for a set of identical images. The poor correlations in this case are due to the image content and effects inherent in the correlation algorithm such as poor predictions and smaller window sizes. The high percentage of good correlations for the Kamloops stereo pair and another test site (Skeena) shows the effectiveness of the two stage parallax measurement scheme.

In order to evaluate the accuracy of these results a profile has been extracted and plotted on Figure 8 as a dotted line on the upper portion of the graph for an arbitrary reference plane. For comparison, the actual elevation extracted from topographic 1:50 000 scale map is represented as a solid line. Absolute calibration has been done with 16 altimetric ground control points used to fit a third order polynomial over the entire DEM. The lower dotted line of Figure 8 represents the altitude after absolute calibration. It differs from the actual relief with a residual error of 150 metres RMS. There is a good agreement between the two curves, however a residual drift of the DEM obtained from LANDSAT has not been corrected by the regression. Another test performed on a second profile, covering 20 kilometres, has shown similar behaviour with an RMS error of 110 metres. Further refinements of the pre-processing of the original images and of altimetric calibration model should improve these results. For complementary information, Figure 9 shows the radiometric values of the stereo images plotted with different offsets along the same profile as Figure 8. The very small misregistration between the two images and the level of noise between their radiometric values demonstrate the sensitivity and robustness of the methodology proposed here.

V APPLICATIONS

Elevation models could be integrated with LANDSAT images in many different ways depending upon the purpose of the applications. As an example, it could be used to improve the geometric rectification of the LANDSAT data in order to generate an orthogonolized image. If we consider a maximum value of 10% for the parallax/height ratio within a full LANDSAT scene, we can see from these preliminary results that relief distortions could be corrected to approximately (10% x 150 metres RMS) 15 metres RMS, upgrading the geometric rectification to subpixel accuracy. The same type of rectification will be considerably more important for new sensors such as the SPOT HRV which will produce greater distortions due to relief in off-nadir images.

Also, as the DEM is in registration with the reference image, we can easily improve the three-dimensional viewing effect by generating a synthetic off-nadir image with a larger slant angle [2]. Figures 10 and 11 show computer generated stereo images for which the equivalent base to height ratio is about 84%. At this level of stereo enhancement, a residual noise could be detectable in rivers, by not exhibiting monotonic elevations. Figures 12 and 13 represent a stereo enhancement of approximately 60% (base to height ratio) over another test site, the Skeena Mountains, in British Columbia. In these stereo images the noise is still perceptable but should not confuse an experienced interpreter. The agreement between the relief perception and the shadows is evident reflecting the good registration between the elevation model and the original image.

VI CONCLUSION

It is shown that digital elevation model can be derived by digital stereo correlation of LANDSAT-MSS stereo pairs. A methodology has been developed with a two stage zoom-in approach and has been shown to be adequate to measure one dimensional parallax between stereo pairs to subpixel accuracy.

This technique could be envisaged for digital stereo correlation of other types of images acquired from future sensors such as the SPOT HRV. The improved stereo capabilities of this sensor would definitely increase the precision of the derived elevation models and facilitate new applications of these models.

ACKNOWLEDGEMENTS

The authors are grateful to Mr. F.E. Guertin, CCRS, for helpful discussions on this research and also to Mr. K. Barkman, CCRS, for providing the input data.

One of the authors, V.G. Krishna acknowledges the assistance of Natural Sciences and Engineering Research Council for the fellowship during the tenure of this research.

REFERENCES

1. Simard, R., 1982.
   Improved Spatial and Altemetric Information from SPOT Composite Imagery. Proceedings of the Intern. Symp. on Remote Sensing of Environment, Second Thematic Conf. "Remote Sensing for Exploration Geology", Dec. 6-10, Fort Worth, Texas.

2. Simard, R., 1983.
   Digital Stereo Enhancement on LANDSAT-MSS Data. Proceedings of the 17th Intern. Symp. on Remote Sensing of Environment, Ann Arbor, MI, May 9-13.

3. Butlin, T.J., F.E. Guertin and S.S. Vishnubhatla, 1978.
   The CCRS Digital Image Correction System. Proceedings of the Fifth Canadian Symposium on Remote Sensing, pp. 271-283.

4. Shlien, S., 1979.
   Geometric Correction, Registration and Resampling of LANDSAT Imagery. Canadian Journal of Remote Sensing, Vol. 5, No. 1.

5. Barnea, D.I. and H.F.Silverman, 1972.
   A Class of Algorithms for Fast Digital Image Registration. IEEE Trans. on Computers, Vol. C21, pp. 179-186. February.

6. Helava, U.V., 1978.
   Digital correlation in photogrammetric Instruments. Photogrammetria, 34, pp. 19-41.

TABLE 1. Correlation Statistics

Images	Good Correlations (%)	Poor Correlations (%)		
		Uniform Window (low variance)	Low Peaks	Multiple Peaks
Identical images	92.6	2.2	0.0	5.2
Kamloops	76.8	1.1	3.2	18.9
Skeena	82.6	3.4	0.2	13.8

Figure 1. MSS band 7 over Kamloops, sub-scene from frame 50-24. Original scale 1:500 000.

Figure 2. MSS band 7 over Kamloops sub-scene from frame 49-24. Original scale 1:500 000.

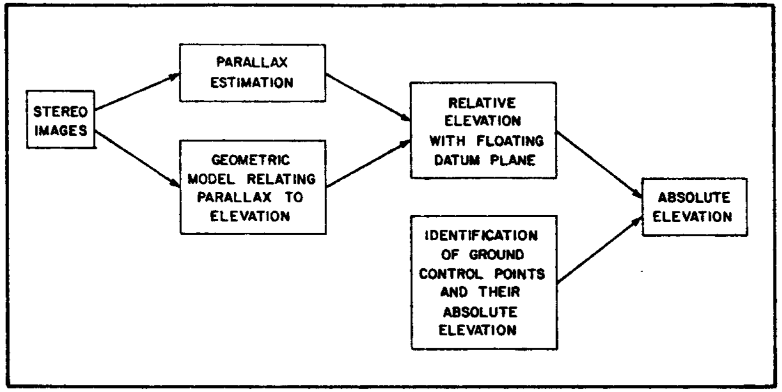

Figure 3. Flow chart of digital elevation modeling process.

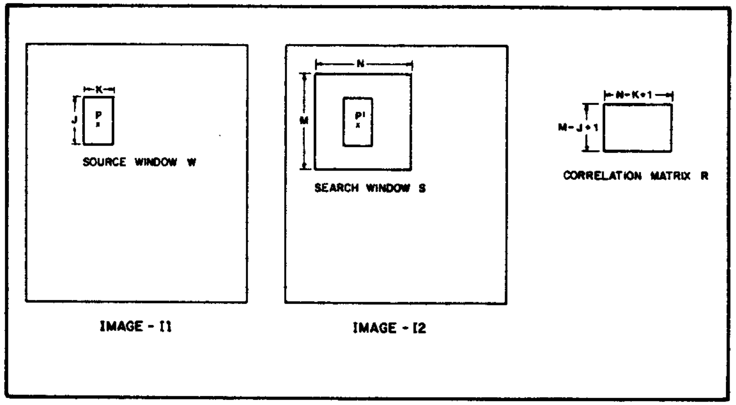

Figure 4. Stereo correlation scheme.

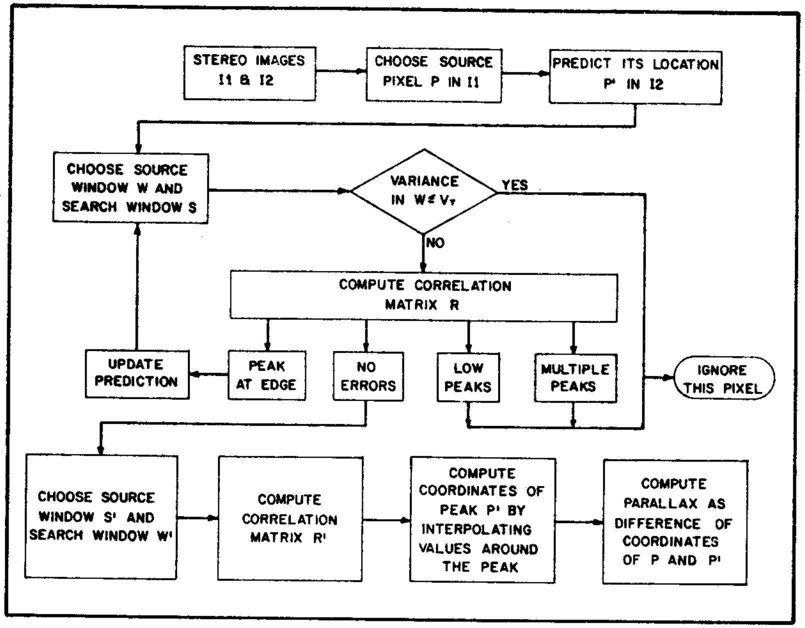

Figure 5. Flow chart of parallax evaluation.

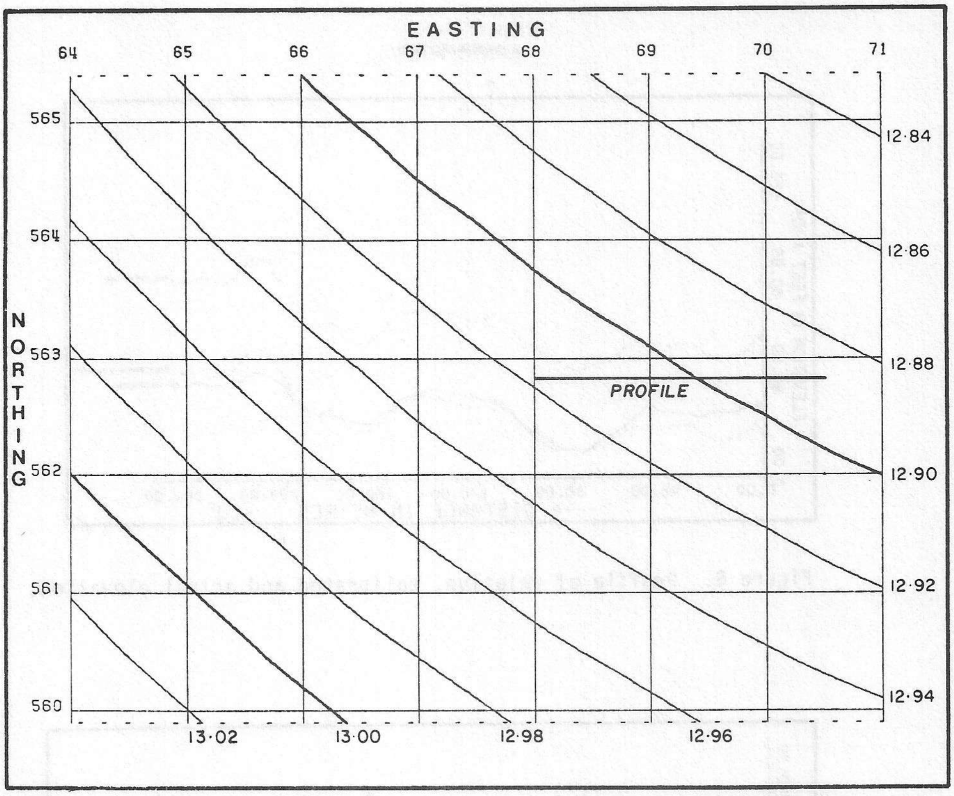

Figure 6. Contour map of the coefficient of the geometric model relating parallax and elevation, increment 0.02%. Original scale 1:500 000. (profile location for Figures 8 and 9).

Figure 7. Density slicing of the relative elevation model, increment 250 m. Original scale 1:500 000. (higher elevations in white).

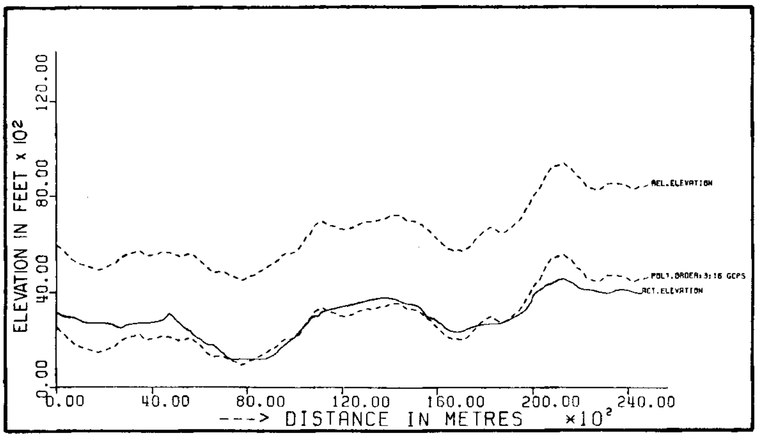

Figure 8. Profile of relative, calibrated and actual elevation.

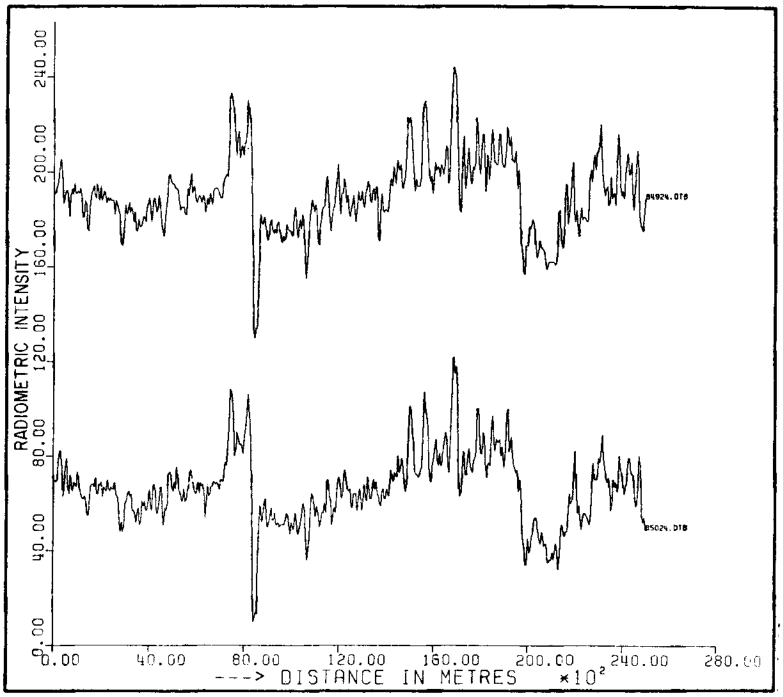

Figure 9. Profile of relative radiometric values for each acquisition.

Figure 10. MSS band 7 over Kamloops, sub-scene from frame 50-24. Original scale 1:500 000.

Figure 11. Simulated off-nadir (slant angle 35° from right) MSS band 7 over Kamloops, sub-scene from frame 50-24. Original scale 1:500 000.

Figure 12. MSS band 7 over Skeena Mountains sub-scene from frame 57-21. Original scale 1:500 000.

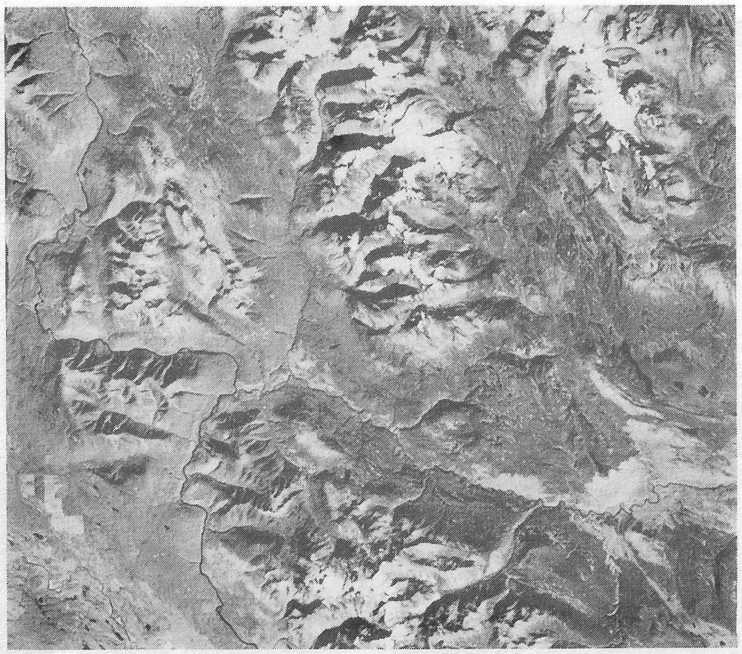

Figure 13. Simulated off-nadir (slant angle 27° from right) MSS band 7 over Skeena Mountains, sub-scene from frame 57-21. Original scale 1:500 000.